Research Article

92

INDONESIAN SCHOLAR SOCIETY

Indones. J. Chem. Stud.
2025, 4(2), 92–100
Available online at journal.solusiriset.com
e-ISSN: 2830-7658; p-ISSN: 2830-778X

Indonesian Journal of Chemical Studies

Adsorption-Desorption of Cd(II) and Mg(II) Ions by Dithizone-Immobilized Coal Bottom Ash

Dwi Putra Wijaya[1]*, Ridho Bonaventura[1], Nurharis Munandar[1], Fajar Hutagalung[1], Chairil Anwar[2]

[1]*Department of Chemistry, Sam Ratulangi University, Manado 95115, Indonesia*

[2]*Department of Industrial Waste Treatment, Politeknik AKA Bogor,Tanah Baru, Bogor 16154, Indonesia*

Received: 25 May 2025; Revised: 7 Aug 2025; Accepted: 8 Oct 2025;
Published online: 24 Dec 2025; Published regularly: 31 Dec 2025

Abstract— Dithizone-immobilized coal bottom ash (DICBA) was successfully prepared as Cd(II) and Mg(II) adsorbent. The parameters examined in the metal ion adsorption study included the effect of pH, adsorbent mass, contact time, and initial concentration. Sequential desorption was examined using H_2O, KNO_3, HNO_3, and Na_2EDTA. The results showed that dithizone had been successfully immobilized on the activated coal bottom ash, as verified by FTIR spectroscopy and XRD analyses. Specific wavenumbers observed included the aromatic group C=C at 1496 cm^{-1}, the C-N group at 1319 cm^{-1} and the Si-O-Si at 1087 cm^{-1} with d-spacing values of 8.313 and 6.046 Å. The optimum conditions for adsorption were 60 min for Cd(II) and 90 min for Mg(II) at a pH of 5 with 0.2 g of adsorbent mass, and an initial concentration of Cd(II) at 50 ppm. The adsorption kinetics of Cd(II) and Mg(II) followed the Ho pseudo-second-order model with 0.174 and 0.285 (g/mol·min) rate constants for Cd(II) and Mg(II), respectively. The highest correlation coefficients (R^2) were 0.995 for Cd(II) and 0.999 for Mg(II). Isotherm modeling indicated that the adsorption of Cd(II) best fitted the Langmuir model (R^2 = 0.988), followed by the Dubinin–Radushkevich (R^2 = 0.952), Freundlich (R^2 = 0.843), and Temkin (R^2 = 0.827) models. The desorption mechanism for Cd(II) and Mg(II) was formed by various interactions, such as physical mechanism (28.25% and 26.26%), ion exchange (23.13% and 14.15%), hydrogen bond formation (16.90% and 12.11%), and mechanism of complex formation (9.56% and 6.13%).

Keywords— *Adsorption-desorption; Cd(II); Coal bottom ash; Dithizone; Mg(II).*

1. INTRODUCTION

With rapid industrial modernization, various toxic metals have been released into the environment as by-products or wastes, leading to harmful effects on living organisms. Pollution in aquatic environments occurs when heavy metals, carried by rainwater from the air, dissolve and enter rivers. In particular, a heavy metal such as cadmium (Cd) has contaminated the water, resulting in environmental degradation and bioaccumulation in both organisms and humans [1-3]. A significant amount of cadmium is absorbed through the respiratory system. This metal has been identified as a carcinogen, and it can affect the prostate, lungs, pancreas, and urinary tract [1]. Regulatory bodies have established permissible limits for cadmium in drinking water to protect public health. The World Health Organization (WHO) recommends a maximum concentration of 0.003 mg/L [4].

Magnesium is a metal that can significantly impact the quality of aquatic systems. Excess concentrations of magnesium ions in aquatic systems can cause various disadvantages. For example, magnesium ions can react with soap, preventing the formation of suds. Additionally, reactions between magnesium ions (Mg^{2+}) in the water also cause crust on the cooking process, which prolongs the boiling process and results in wasted fuel. Therefore, the pollution of heavy metal ions in water should be handled to minimize the effect on human health. Adsorption has long been recognizeed as one of the simplest and most cost-effective method to remove pollutants from water, particularly in large scale, such as in industrial wastewater treatment. There is a need for selective adsorbents with strong affinity for Cd(II) ions with the presence of Mg(II) ions, which can be accomplished by modifying the surface of coal bottom ash that contain specific functional groups. Recent advancements in research have led to the creation of technologies aimed at eliminating heavy metals from industrial wastewater. Effective solutions

***Corresponding author**.
Email address: Putra4570@gmail.com
DOI: 10.55749/ijcs.v4i2.76

for heavy metal removal include electrochemical processes, ion exchange, reverse osmosis, chemical precipitation, coagulation-flocculation, ultrafiltration, photocatalysis, and membrane-based methods [5-6]. Original coal bottom ash is not a selective adsorbent material because its active sites are siloxane, silanol groups and alumina. Hence its adsorption is mainly dominated by electrostatic interaction and even weaker physical interactions. Therefore, to enhance coal ash as a selective adsorbent for Cd(II) and Mg(II) ions, its surface should be modified to incorporate active groups that can easily form chelate complexes with these two metals [7-8]. Dithizone offers distinct advantages for analyzing Cd(II), including high selectivity, good stability, and sensitivity. Dithizone shows high selectivity toward Cd(II) ions due to its strong affinity and the formation of stable, and easily extractable chelates, making it an excellent choice for detection and analysis [9].

In this study, the effectiveness of Dithizone-Immobilized Coal Bottom Ash (DICBA) an adsorbent is evaluated for removing Cd(II) and Mg(II) ions from aqueous solutions. The main factors affecting the adsorption process, including pH, adsorbent mass, contact time, and initial concentration of Cd(II), are systematically examined. Additionally, adsorption kinetics and isothermal models are analyzed. To gain deeper insight into the interaction between Cd(II) ions and the active sites of DICBA, sequential desorption studies are conducted using various solvents, H_2O, KNO_3, HNO_3, and Na_2EDTA.

2. EXPERIMENTAL SECTION

2.1. Materials

The chemicals used in this study were pro analyst (p.a.) grade obtained from Merck: Dithizone; Ethanol 99%; HCl 37%; Toluena; Magnesium Sulfate ($MgSO_4 \cdot 7H_2O$); Cadmium Sulphate ($CdSO_4 \cdot H_2O$); Potassium Nitrate (KNO_3)0.1 M; Nitric Acid (HNO_3)0.001 M; Na_2EDTA 0.1 M, and aquadest. Coal bottom ash was sourced Pacitan plant.

2.2. Instrumentations

The concentration of Cd(II) and Mg(II) ions in solution was quantified with Atomic Absorption Spectrophotometers (AAS Analytik Jena contrAA 300). The crystalline structure and functional groups analysis were performed using a Shimadzu Infrared Spectrometer FTIR 8201 model and X-ray Diffractometer Rigaku miniflex 600, respectively.

2.3. Activation of Coal Bottom Ash

Coal bottom ash was activated grinding and sieving to a particle size of 250 mesh. The activation process involved refluxing 20 g of coal bottom ash in 120 mL of HCl 6 M for 4 h. The solution was filtered and washed with aquadest until the filtrate was neutral. The solids obtained were then dried at 160 °C for 6 h. Activation results were characterized using FTIR.

2.4. Dithizone-Immobilized Coal Bottom Ash (DICBA) Synthesis

The DICBA was prepared by refluxing 4 g of activated coal bottom ash and 1.03 g of dithizone in 80 mL toluene. The solution was filtered and washed with toluene, ethanol and aquadest until there were no dithizone characteristics. The obtained solids were dried in an oven at a 70 °C for 6 h. Immobilization results were characterized using XRD and FTIR.

2.5. Effect of pH

A metal solution containing a mixture of two metal ions, each 30 mL Cd(II) and Mg(II), with a concentration of 50 ppm, was added with 0.1 g of dithizone-immobilized bottom ash. The pH of the solution was varied at pH 3-7. The adsorption process was carried out for 60 min. The adsorbents were filtered, and the metal content in the filtrate was analyzed using an atomic absorption spectrophotometer. This procedure was also applied to the activated bottom ash and without adsorbent, under the same conditions.

2.6. Effect of Adsorbent Mass Variation

A metal solution containing a mixture of two metal ions, each 30 mL Cd(II) and Mg(II) with a concentration of 50 ppm, was added with variations in the adsorbent mass of 0.05; 0.1; 0.2; 0.3; 0.4; and 0.5 g of DICBA at optimum pH solution. The adsorption process was carried out for 60 min. The adsorbents were filtered, and the metal content in the filtrate was analyzed using an AAS.

2.7. Effect of Time Variation

The effect of contact time between adsorbent and adsorbate on the effectiveness of the adsorption was investigated in the range of 5–90 min. A solution containing 30 mL Cd(II) and Mg(II) with a concentration of 50 ppm was added with 0.2 g of DICBA at optimum pH solution. The adsorption process was carried out with time variations of 5; 15; 30; 45; 60 and 90 min. The adsorbents were filtered, and the metal content in the filtrate was analyzed with an AAS.

2.8. Effect of Initial Concentration

The initial concentration of metal ions varied in the 10–100ppm range. A metal solutions containing of Cd(II) and Mg(II) of 30 mL with a concentration of Mg(II) was maintained at 50 ppm and the initial concentration of Cd(II) was varied at 10; 25; 50; 75; 100 ppm. The mixed solution was added with 0.2 g of DICBA at optimum pH solution. The adsorption process was carried out for 60

min. The adsorbents were filtered, and the metal content in the filtrate was analyzed using an AAS.

2.9. Desorption Study

The adsorbed precipitate was further dried for sequential desorption with various solutions, such as 10 mL H_2O, 10 mL 0.1 M KNO_3, 10 mL 0.001 M HNO_3, and 10 mL 0.001 M Na_2EDTA. The desorption of the adsorbed metal ions was conducted by sequentially stirring the adsorbent with adsorbed metal ions in 10 mL of each solvent with a contact time of 60 min for each desorption solvent.

3. RESULT AND DISCUSSION

3.1. Preparation of DICBA

The basic characterization before and after activation characterized conducted by an FTIR to analyze the functional groups present in the adsorbent. Infrared spectra before and after activation are presented in **Fig. 1.** The spectra show the wide absorption wavenumber at 3425 cm^{-1}, indicating the presence of vibration of OH on Si-OH and water molecules in coal bottom ash. This absorption is amplified by the vibration of O-H bending at the wavenumber 1620 cm^{-1}. The 1087 cm^{-1} and 794 cm^{-1} wavenumbers are the implication of the Si-O stretching vibration of the Si-O-Si and Si-O-Al groups from the coal bottom ash [10].

Characterization of DICBA was carried out by FTIR instrument to determine the change of functional group after immobilized with dithizon compared with activated bottom ash. The infrared spectra showing immobilization are presented in **Fig. 1(c).** The results showed the characteristics of the dithizone appearing on the DICBA. This indicates that the immobilization of dithizone has been successfully performed on activated coal bottom ash. The observed two absorbent characteristic bands of dithizone did not appear on the activated bottom ash spectra. The two absorption bands are the vibrational absorption of the C=C aromatic group of the phenyl group (1496 cm^{-1}) and the vibrational uptake of the C-N group (1319 cm^{-1}) of dithizone. The absorption bands from the vibration of the C=S group (1200-1050 cm^{-1}) were not identified in this study, because the absorption band is allegedly fused with a strong and wide absorption band from the Si-O-Si (1087 cm^{-1}) wavenumber group [11].

Characterization of dithizone-immobilized bottom ash was also carried out by an X-ray diffractometer to support the characterization result of the dithizone-immobilize process on the activated bottom ash with FTIR. Diffractograms on coal bottom ash before and after immobilization are shown in **Fig. 2.**

The results of the diffractogram can be interpreted by comparing the values of the d-spacing main peak that appears on the activated bottom ash and dithizone-immobilized bottom ash to know the characteristics of dithizone. Based on the results of the main peak interpretation of the dithizone-immobilized bottom ash, the characteristics of dithizone have been identified on DICBA spectra. This indicates that the immobilization of dithizone has been successfully performed on activated coal bottom ash.

The peaks that prove that coal bottom ash has immobilized with dithizone appear on d-spacing 8.313 and 6.046 Å, corresponding to the characteristic d-spacing peaks of the dithizon compound (8.31, 6.05, and 4.71 Å) [12]. The characteristic of the dithizone on immobilized coal bottom ash is seen only slightly. This is because the peak of the dithizone and the top of the coal bottom ash are stacked together so that the peak shows the characteristics of the bottom ash at 4.26, 3.35, 2.45, and 1.818 Å, which is the peak of quartz, while the mullite peak appears at 3.713 and 1.529 Å. The immobilization of dithizone to the activated coal bottom ash surface does not significantly alter the coal bottom ash diffraction pattern. Thus, it can be concluded that immobilization does not alter the structure and crystallinity of the adsorbent.

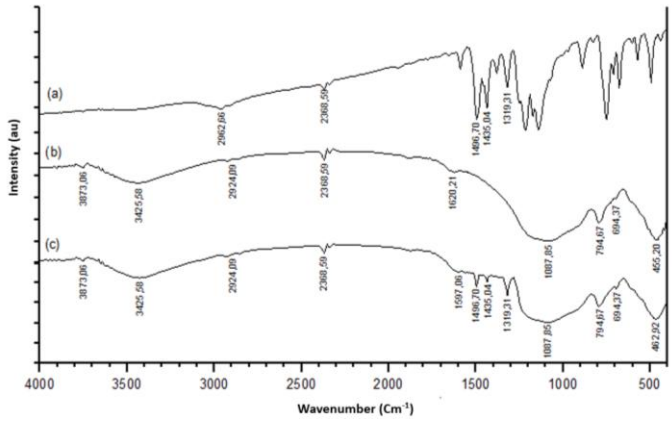

Fig. 1 Infrared spectra of (a) dithizone, (b) activated coal bottom ash, and (c) DICBA

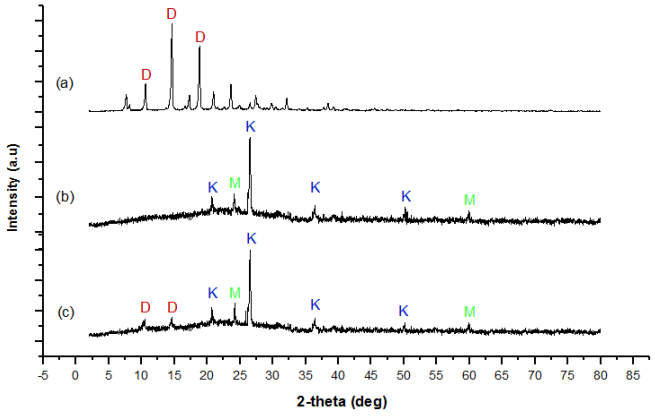

Fig. 2 The XRD diffractogram of (a) dithizone, (b) coal bottom ash before immobilization, and (c) after immobilization

3.2. Effect of pH Solution

The results of pH variation of Cd(II) and Mg(II) adsorption on DICBA are shown in **Fig. 3.** The data shows that at different pH levels, the amount of metal ion adsorbed is also different. The pH of this solution may affect the adsorption capacity of the adsorbent for the metal ion. **Fig. 3** shows that the adsorbed metal ion was increases with the increasing of the pH.

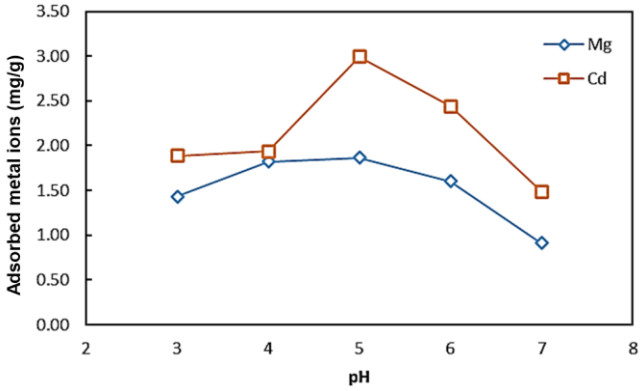

Fig. 3 Effect of pH on adsorbed Cd (II) and Mg (II) ions onto dithizone-immobilized coal bottom ash

The pH of the optimum for the dithizone-immobilized bottom ash occurs at pH 5 with the adsorbed Cd(II) and Mg(II) were 2.99 mg/g and 1.86 mg/g, respectively. The pH of the medium has an essential effect on the interaction between the adsorbent surface and the metal ions. The solution with low pH was in the form of a metal cation with a +2 oxidation number. At pH 7, the adsorption of Cd(II) and Mg(II) ions decreased to the lowest level, i.e. 1.48 mg/g and 0.91 mg/g, respectively. The pH affect the ability of the adsorbent to bind to the metal cation [12,13]. At the optimum condition (pH 5.0), the number of metal ions interacting with the active site of the adsorbent reaches the maximum amount [14]. This is due to the pH that indicates the amount of H^+ ions in the solution is decreasing, whereas the presence of OH^- ions is still insufficient to precipitate metal ions [15].

3.3. Effect of Adsorbent Mass Variation

The effect of variation of adsorbent mass are presented in **Fig. 4.** There was an increase in the amount of metal ions adsorbed in line with the increase in mass of adsorbent used. An increase in the number of adsorbed metal ions is equivalent to the number of active sites of the adsorbent when the mass of the adsorbent increases until some point [16].

The optimum mass adsorbent on the adsorbed Cd(II) and Mg(II) was 0.2 g. After reaching the optimum mass at 0.72 and 0.62 mg/g for Cd(II) and Mg(II), respectively. This result shows that the adsorbed ions in the solution have reached the equilibrium condition, so that the increase of adsorbents did not change the amount of adsorbed metals [17]. As most of the available binding sites are already filled, the saturation of active sites on the adsorbent surface restricts any additional adsorption, causing the adsorption capacity to level off after the optimal adsorbent dosage is reached. The adsorption ability of both adsorbents tends to decrease slightly during the desorption process due to stirring process.

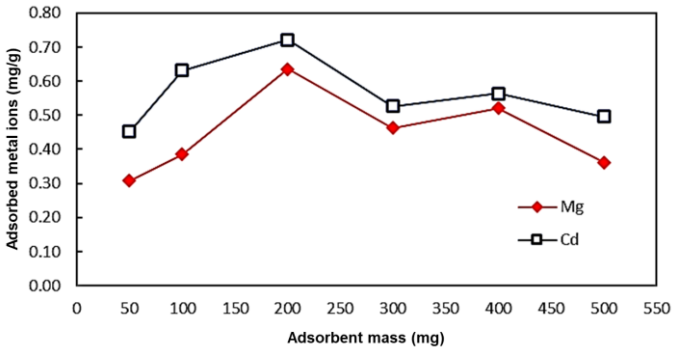

Fig. 4. Effect of adsorbent mass on adsorbed Cd(II) and Mg(II) on dithizone-immobilized coal bottom ash

3.4. Effect of Adsorption Time Variation

The results of the Cd(II) and Mg(II) adsorption on dithizone-immobilized coal bottom ash are presented in **Fig. 5.** Based on the results, it is shown that the interaction time affects the amount of metal ions that can be absorbed by an adsorbent. The amount of adsorbed metal ions increases due to the increase in contact time to reach the optimum time. The optimum time of Cd(II) and Mg(II) adsorption on dithizone-immobilized coal bottom ash is 60 and 90 min, respectively. The increase in the amount of metal ions adsorption capacity is due to a longer chance of interaction between the metal ion and the adsorbent sites in solution [18].

Chemical kinetics research provides crucial knowledge about the adsorption rate and the variables influencing it [19]. The investigation of the controlling rate Cd(II) and Mg(II) adsorption was assessed by

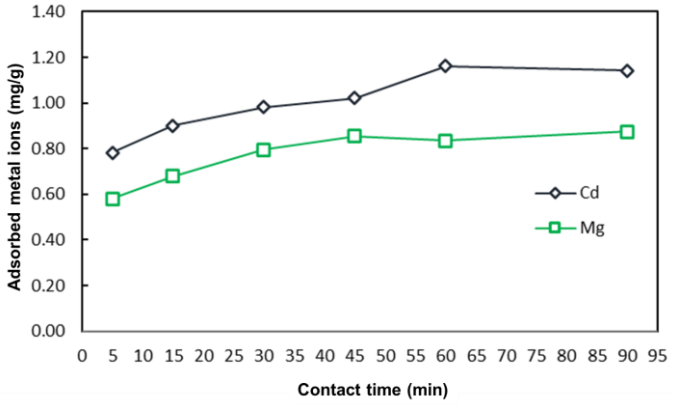

Fig. 5. Effect of contact time of Cd(II) and Mg(II) adsorption on DICBA

Lagergren (pseudo-first-order) (1), Ho (pseudo-second-order) (2), Weber-Morris IPD (3), Elovich (4), Santosa (5), and Rusdiarso-Basuki-Santosa (RBS) (6). **Table 1** shows that Cd(II) and Mg(II) adsorbtions follow the Ho second-pseudo order, with the value of the rate constant, kHo, was 0.174 and 0.285 (g/mol min) for Cd(II) and Mg(II), respectively. The linear plots of Lagergren, Ho, Santosa, Elovich, RBS, and Waber-Morris IPD are shown in **Fig. 6**. Based on the correlation coefficient (R^2) value, the Ho pseudo-second-order kinetic model gives the best plotting models with R2=0.9948 and 0.9988, for Mg(II) and Cd(II), respectively.

$$\ln(_{qe} - _{qt}) = \ln q_e - k_{lag}t \quad (1)$$

$$\frac{t}{q_t} = \frac{1}{k_{Ho}(q_e^2)} + \frac{1}{q_t}t \quad (2)$$

$$qt = k_{IP}t^{1/2} + Ci \quad (3)$$

$$q_t = \frac{1}{\beta}\ln(\alpha\beta) + \frac{1}{\beta}\ln(t) \quad (4)$$

$$\frac{1}{(C_o - Xq_e)}\ln\left(\frac{q_e(C_o - Xq_t)}{C_o(q_e - q_t)}\right) = k_s t \quad (5)$$

$$\ln\left(\frac{C_oC_b - X_eX}{X_e - X}\right) = k_a\left(\frac{C_oC_b - X_e^2}{X_e}\right)t - \ln\left(\frac{Xe}{C_oC_b}\right) \quad (6)$$

The adsorption rate constants k_{lag} (min^{-1}), k_{Ho} (g/mol.min), k_{IP} ($mg/g.min^{1/2}$), k_S (L/mol.min), and k_a (L/mol.min) correspond to the Lagergren, Ho, Weber–Morris intraparticle diffusion (IPD), Santosa, and RBS kinetic models, respectively. The constant Ci in the Weber–Morris model reflects the boundary layer effect during the adsorption process. The Elovich model parameter α (mg/g·min) represents the initial adsorption rate, indicating how fast adsorption begins, while β (g/mg) is the desorption constant, associated with surface coverage and the activation energy of chemisorption. The parameters q_e and q_t (mol/g) shows the amount of Cd(II) and Mg(II) ions adsorbed at equilibrium. C_0 (mol/L) and C_b (mol/L) refer to the initial and equilibrium concentrations of Cd(II) or Mg(II) in the solution, when using dithizone-immobilize coal bottom ash as the adsorbent.

Similarly, x (mol/L) and xe (mol/L) indicate the amount of Cd(II) or Mg(II) adsorbed on the active sites using dithizone-immobilized coal bottom ash at time t and at equilibrium. In Santosa's kinetic model, X (g/L) is defined as *w/vmr*, where *w* is the mass of the adsorbent (g), *v* is the volume of the adsorption solution (L), and *mr* is the molar mass of the adsorbate. Finally,

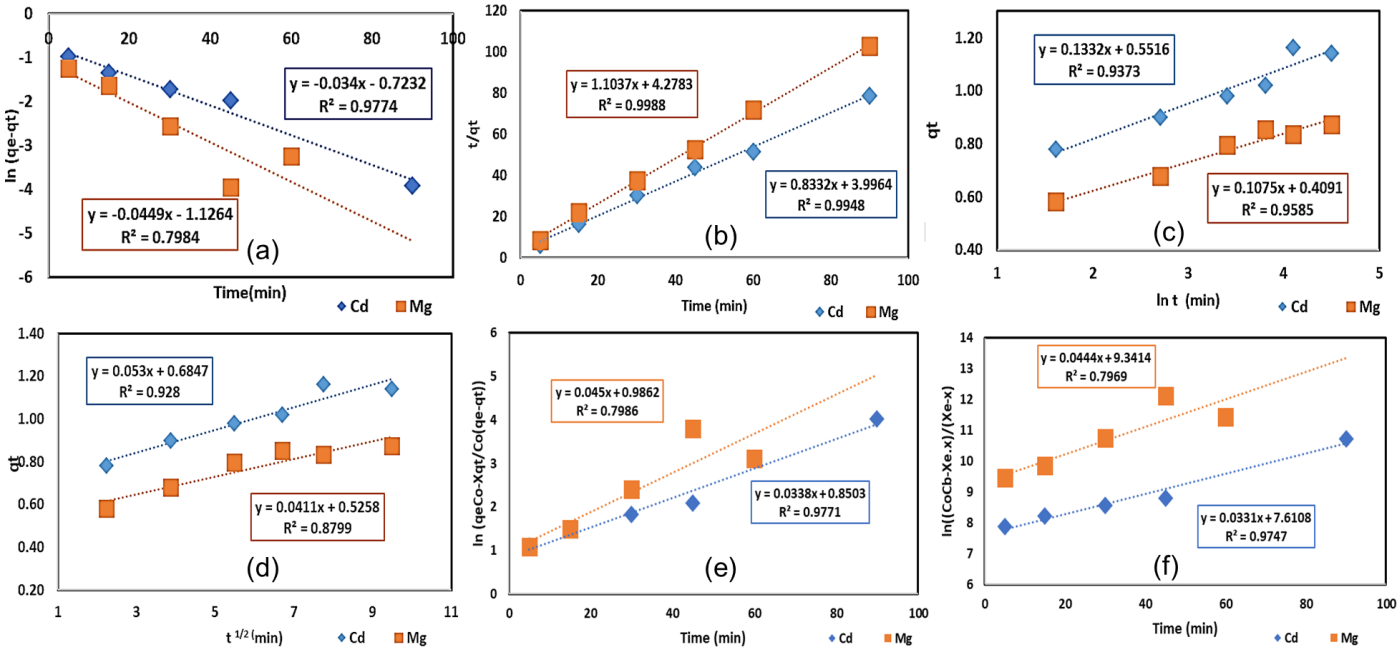

Fig. 6. Linear plot of (a) Lagergren, (b) Ho, (c) Elovich, (d) Weber-Morris IPD, (e) Santosa, and (f) RBS kinetics model of Mg(II) and Cd(II) adsorption on DICBA

Cb (mol/L) represents the Langmuir adsorption capacity, calculated from *bw/v*. [12].

Fig. 5 shows that the optimum contact time for equilibrium to be achieved in the interaction between metal ions and the active site on the adsorbent. The amount of adsorbed ions will equal the amount of dissolved metal ions when equilibrium is reached [20]. The adsorption capacity tends to remain due to the saturated surface condition of the adsorbent, so that the adsorbent can not absorb the metal ions even with the increase of the contact time [6].

Table 1. Kinetics parameters of Cd(II) and Mg(II) adsorption onto DICBA

Kinetics Parameters	Cd(II)	Mg(II)
Lagergren		
k_{Lag} (min^{-1})	0.034	0.045
R^2	0.977	0.798
Ho		
k_{Ho} (g/mol. min)	0.174	0.285
R^2	0.995	0.999
Weber-Morris (IPD)		
k_{IP} ($mg/g.min^{1/2}$)	0.053	0.041
R^2	0.928	0.880
Elovich		
α ($mg\ g^{-1}\ min^{-1}$)	8.37	4.84
β ($g\ mg^{-1}$)	7.509	9.302
R^2	0.937	0.959
Santosa		
k_s (L/mol.min)	0.034	0.045
R^2	0.799	0.977
RBS		
k_a ($10x^{-5}$ L/mol.min)	4.09	1.07
R^2	0.797	0.975

3.5. Effect of Initial Concentration

The results of simultaneous adsorption of Cd(II) on DICBA with variation of initial concentration of Cd(II) are presented in **Fig. 7**. It shows that the amount of adsorbed metal ions increases as the initial concentration of Cd(II) increases and tends to remain after the initial concentration reaches 75 ppm. The adsorption of the Cd(II) metal ion using dithizone-immobilized coal bottom ash reached an optimum at an initial concentration of Cd(II) of 50 ppm.

After reaching the optimum conditions, the adsorption of metal ions Cd(II) tends to decrease. This is due to the presence of Cd(II) ions adsorbed on the surface of the adsorbent. The tendency of decreased adsorbed Cd(II) was also caused by the condition of the adsorbent surface, which has reached saturation, so the adsorbent can not adsorb the Cd(II) even though the concentration of Cd(II) was increasing [21]. Initial concentration variations of Cd(II) ion can be used to determine the isotherm adsorption model of Cd(II) ion on the dithizone-immobilized coal bottom ash. The

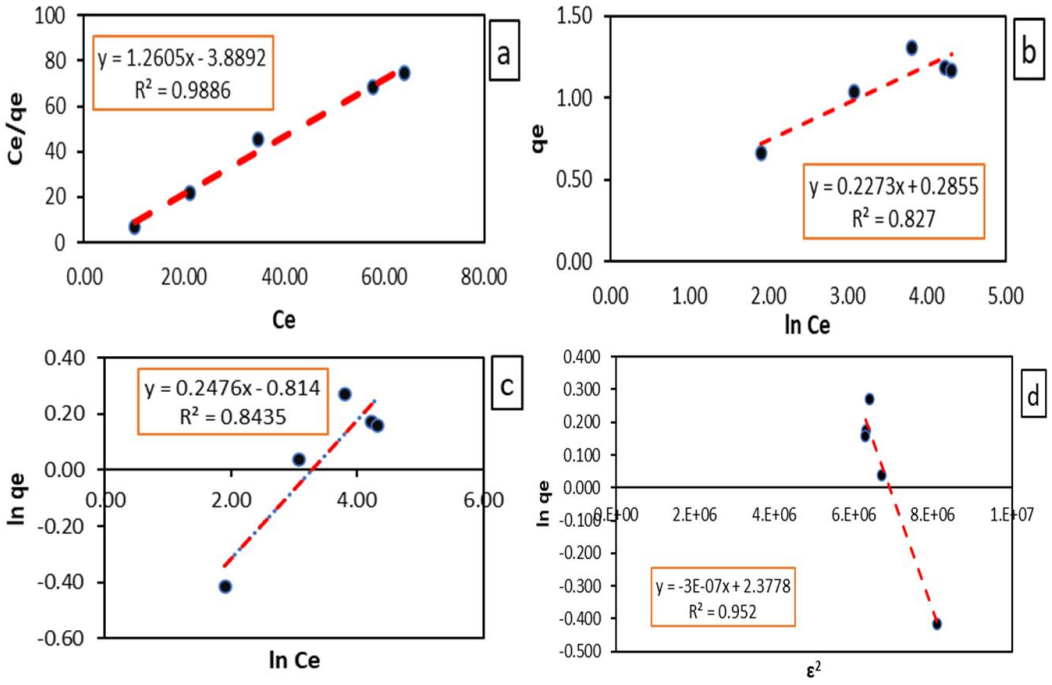

Fig. 7 Isotherm models of (a) Langmuir, (b) Tempkin, (c) Freundlich and (d) DR of Cd(II) adsorption onto DICBA

adsorption isotherm is used to determine the interaction between the solution with the adsorbent and the adsorption capacity [22].

The isotherm of adsorption studies in this research was evaluated by the Langmuir, Freundlich, Temkin, and Dubinin-Radushkevich (DR) isotherms models. The results of correlation coefficient (R^2) of langmuir, Freundlich, Temkin, and Dubinin-Radushkevich (DR) equation were 0.988, 0.843, 0.827, and 0.952, respectively (**Fig. 7**). The parameters used in the comparison are those giving the best plotting isotherm parameters is the Langmuir isotherm model. The Langmuir model involves the formation of a chemical bond between the adsorbate molecule and the surface of the adsorbent. A strong chemical bond can cause the formation of a single layer of adsorbate on the surface of the adsorbent. The immobilization of coal bottom ash enhances the adsorption capacity and selectivity for Cd(II) ions. The isotherm parameters of Cd(II) adsorption on dithizone-immobilized coal bottom ash are presented in **Table 2.**

Table 2. Isotherm parameters of Cd(II) adsorption onto dithizone-immobilized coal bottom ash

Isotherm Parameters	Cd (II)
Langmuir	
b (mol/g)	1.043×10^{-5}
K_L (L/mol)	13,125.6
E_L (kJ/mol)	25.124
R^2	0.988
Freundlich	
B (mg/g)	0.44
n	4.04
R^2	0.843
Dubinin-Radushkevich DR	
q_{DR}(mg/g)	10.77
B_{DR} (mol^2/J^2)	3×10^{-7}
E_{DR} (kJ/mol)	7.74×10^{-4}
R^2	0.952
Temkin	
b_T (J/mol)	107.1
A_T (L/g)	3.52
R^2	0.827

3.6. Desorption Study

The study reveals the interactions that occur between metal ions and adsorbents. Sequential desorption was performed gradually using Aquadest, KNO_3, HNO_3, and Na_2EDTA solvents (**Fig. 8**). Desorption with aquadest was performed to determine the presence of Van der Waals bonds between the adsorbent and the metal ions. The results showed that the amount of Cd(II) and Mg(II) ions desorbed using aquadest was 28.25 and 26.26%, respectively. This result indicates that the adsorption process of Cd(II) and Mg(II) occurs primarily through physical interaction involving the Van der Waals bond. These bonds arise from dipole-dipole interactions caused by the transfer of electrons between molecules [23].

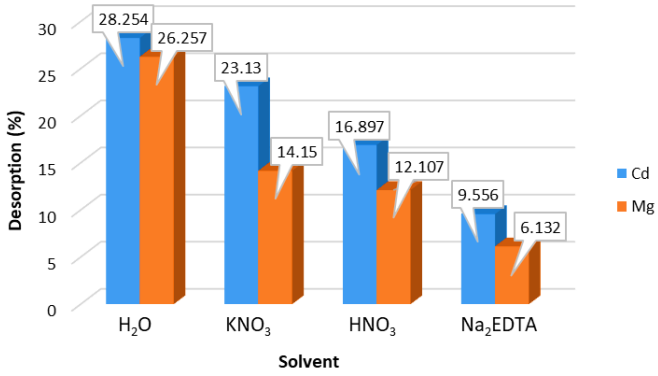

Fig. 9 Desorption results of Cd(II) and Mg(II) ions on DICBA

Based on the desorption conducted using KNO_3, the removal efficiencies for Cd(II) and Mg(II) ions were observed to be 23.13% and 14.15%, respectively. The purpose of using KNO_3 as a desorption solvent is to investigate the existence of ionic bonds and cation exchange between KNO_3 and Cd(II) and Mg(II) metal ions. The interaction between metal ions and adsorbents is dominated by physical and electrostatic interactions because water and KNO_3 yield the highest desorption results. The bonds through ion exchange are strong bonds because KNO_3 solvent effectively releases Cd(II) and Mg(II) ions [24].

Desorption using an HNO_3 solvent is used to determine the formation of hydrogen bonds in the adsorption process. The desorption results revealed mass percentages of 16.90% and 12.11% for Cd(II) and Mg(II) metal ions, respectively. The acquisition of a percent desorption value using an HNO_3 solvent shows that hydrogen formation interaction occurs in the adsorption process of Cd(II) and Mg(II) metal ions. Upon hydration, metal ions form hydration complexes, which promotes the development of hydrogen bonds with the adsorbent's active sites. The water ligands associated with the hydrated metal ions may interact through hydrogen bonding with the functional groups present on the adsorbent surface [25].

The desorption process using Na_2EDTA revealed that 9.56% of Cd(II) ions and 6.13% of Mg(II) ions were dissolved. The purpose of using Na_2EDTA for desorption is to determine the potential of complex formation between Cd(II) and Mg(II) ions with Na_2EDTA. Since complex formation is a strong bond, the release process of these ions is not straightforward. The percent value of desorption using a small Na_2EDTA solvent indicates that the interaction of Cd(II) and Mg(II) ions through complex formation is relatively weak compared to the physical and ionic interactions.

CONCLUSION

The DICBA has been successfully synthesized by refluxing dithizon on the activated coal bottom ash using toluene as a solvent. This synthesis was confirmed with FT-IR and XRD. The specific wavenumbers identified were C=C aromatic group of the phenyl group (1496 cm^{-1}), the vibrational uptake of the C-N group (1319 cm^{-1}) of dithizone, and Si-O-Si (1087 cm^{-1}) from the coal bottom ash. In addition, the characteristic d-spacing of 8.313 and 6.046 Å correspond to the notable d-spacing peaks of the dithizon compound (8.31; 6.05; and 4.71 Å), indicating that dithizon-immobilized coal bottom ash was successful. The optimum conditions for the adsorption of Cd(II) and Mg(II) ions on the immobilized dithizon coal bottom ash were at pH 5, with a 0.2 g adsorbent mass. Under these conditions, the adsorption capacities were measured at 0.72 and 0.62 mg.g^{-1} for Cd(II) and Mg(II) metal ions, respectively, using an initial concentration of 50 ppm of Cd(II) and contact times of 60 and 90 min. The adsorption kinetics for Cd(II) and Mg(II) metal ions adhered to the Ho pseudo-second-order kinetics, with rate constants of 0.174 and 0.285 (g/mol·min) for Cd(II) and Mg(II), respectively. The adsorption isotherm parameters for Cd(II) primarily followed the Langmuir and DR adsorption isotherm models, with linear regression correlation coefficients (R^2) of 0.988 and

0.952, respectively. The simultaneous adsorption mechanism for Cd(II) and Mg(II) ions was influenced by various factors: physical mechanisms accounted for 28.26% and 26.26%, ion exchange mechanisms for 23.06% and 14.14%, hydrogen bonding mechanisms for 16.83% and 12.12%, and complex forming mechanisms for 9.59% and 6.06%. The desorption results for Cd(II) and Mg(II) ions were dominated by physical and electrostatic interactions, with water and KNO_3 yielding the highest desorption percentages.

SUPPORTING INFORMATION

There is no supporting information in this paper. Data supporting this research's findings are available upon request from the corresponding author (DPW).

ACKNOWLEDGEMENTS

We would like to thanks to the Sam Ratulangi University for the instrumentation support.

CONFLICT OF INTEREST

The authors declare that there was no conflict of interest in this study.

AUTHOR CONTRIBUTIONS

DPW: Data curation, Formal analysis, Investigation, Resources, Software, Visualization, Writing original draft. RB: Conceptualization, Methodology, Administration. Nurharis Munandar: Supervision, Validation, Review & editing. Fajar Hutagalung: Writing original draft, review, editing. CA: Writing original draft, Conceptualization, Funding acquisition, Methodology, Supervision, Visualization. All authors agreed to the final version of this manuscript.

REFERENCES

[1] Vajargah, M.F. 2021. A review on the effects of heavy metals on aquatic animals. *J. Biomed. Res. Environ. Sci.* 2(9). 865-869. doi: 10.37871/jbres1324

[2] Jais, N., Ikhtiar, M., Gafur, A., & Abbas, H.H., 2020. Bioaccumulation of Heavy Metals Cadmium (Cd) and Chromium (Cr) Found in Water and Fish in the Tallo River Makassar. *Window of Public Health Journal*. 1(3). 261-273. doi: 10.33096/woph.v1i3.65

[3] Cordova, M.R. 2021. A preliminary study on heavy metal pollutants chrome (Cr), cadmium (Cd), and lead (Pb) in sediments and beach morning glory vegetation (ipomoea pes-caprae) from dasun estuary, Rembang, Indonesia. *Mar. Pollut. Bull.* 162. 111819. doi: 10.1016/j.marpolbul.2020.111819

[4] World Health Organization (WHO). 2017. *Guidelines for Drinking-water Quality*. Fourth Edition Incorporating the First Addendum. Geneva: World Health Organization.

[5] Huda, B.N., Wahyuni, E.T., Mudasir, M., 2021. Eco-friendly immobilization of dithizone on coal bottom ash for the adsorption of lead(II) ion from water. *Results Eng.* 10. 100221. doi: 10.1016/j.rineng.2021.100221

[6] Mudasir, M., Karelius, K., Aprilita, N.H., Wahyuni, E.T. 2016. Adsorption of mercury(II) on dithizone-immobilized natural zeolite. *J. Environ. Chem. Eng.* 4. 1839-1849. doi: 10.1016/j.jece.2016.03.016

[7] Dong, Y., Zhou, M., Xiang, Y., Wan, S., Li, H., & Hou, H. 2019. Barrier effect of coal bottom ash-based geopolymers on soil contaminated by heavy metals. *RSC Adv.* 9(42). 28695-28703. doi: 10.1039/c9ra05542h

[8] Fitriana, D., Mudasir, M., Siswanta, D. 2020. Adsorption of Pb(II) from aqueous solutions on dithizone-immobilized coal fly ash. *Key Eng. Mater.* doi: 10.4028/www.scientific.net/kem.840.57

[9] Basuki, R., Apriliyanto, Y., Stiawan, E., Pradipta, A.R., Rusdiarso, B., & Putra, B.R. 2025. Magnetic hybrid chitin-horse manure humic acid for optimized Cd(II) and Pb(II) adsorption from aquatic environment. *Case Stud. Chem. Environ. Eng.* 11. 101138. doi: 10.1016/j.cscee.2025.101138

[10] Huang, J., Yuan, F., Zeng, G., Li, X., Gu, Y., Shi, L., Liu, W., Shi, Y. 2017. Influence of pH on heavy metal speciation and removal from wastewater using micellar-enhanced ultrafiltration. *Chemosphere*. 173. 199-206. doi: 10.1016/j.chemosphere.2016.12.137

[11] Tajudin, W.S., Sunarti, S., & Manuhutu, J. B. (2023). Optimasi Massa Adsorben Dan pH Pada Adsorpsi Ion Fe Menggunakan Abu Cangkang Kelapa Sawit. *Molluca Journal of Chemistry Education*. 13(2). 74-86. doi: 10.30598/MJoCEvol13iss2pp74-86

[12] Krisdiyanto, D., Khamidinal, & Faqih, A. 2022. Adsorption Cd (II) by Zeolite from Bottom Ash Modified by Dithizone. *J. Trop. Chem. Res. Edu.* 4(2). 110-125. doi: 10.14421/jtcre.2022.42-06

[13] Basuki, R., Santosa, S.J. and Rusdiarso, B. 2017. Ekstraksi adsorben ramah lingkungan dari matriks biologi: asam humat tinja kuda (AH-TK). *Chempublish J.* 2(1). 13-25.

[14] Sari, M.K., Basuki, R. and Rusdiarso, B., 2021. Adsorption of Pb(II) from aqueous solutions onto humic acid modified by urea-formaldehyde: Effect of pH, ionic strength, contact time, and initial concentration. *Indones. J. Chem.* 21(6). 1371-1388. doi: 10.22146/ijc.64600

[15] Ngatijo, N., Gusmaini, N., Bemis, R. and Basuki, R. 2021. Adsorption of methylene blue on humic acid coated magnetite nanoparticles: isotherm and kinetic study. *Chemical Engineering Research Articles*. 4(1). 51-64. doi: 10.25273/cheesa.v4i1.8433.51-64

[16] Basuki, R., Yusnaidar, Y. and Rusdiarso, B. 2018. Different style of Langmuir isotherm model of non-competitive sorption Zn(II) and Cd(II) onto horse dung humic acid (HD-HA). *AIP Conf. Proc.* 2026(1). 020009. doi: 10.1063/1.5064969

[17] Basuki, R., Santosa, S.J. and Rusdiarso, B. 2017. The novel kinetics expression of Cadmium(II) removal using green adsorbent horse dung humic acid (HD-HA). *AIP Conf. Proc.* 1823(1). 020001. doi: 10.1063/1.4978074

[18] Ngatijo, N., Permana, E., Yanti, L.P., Ishartono, B. and Basuki, R., 2021. Remazol briliant blue uptake by green and low-price black carbon from ilalang weeds (*Imperata cylindrica*) activated by KOH solution. *JKPK (Jurnal Kimia dan Pendidikan Kimia)*. 6(2). 192-205. doi: 10.20961/jkpk.v6i2.53113

[19] Ngatijo, N., Basuki, R., Nuryono, N. and Rusdiarso, B. 2019. Comparison of Au(III) Sorption on Amine-Modified Silica (AMS) and Quaternary Amine-Modified Silica (QAMS): A Thermodynamic and Kinetics Study. *Indones. J. Chem.* 19(2). 337-346. doi: 10.22146/ijc.33758

[20] Basuki, R., Rusdiarso, B., Santosa, S.J., Siswanta, D. 2021. The dependency of kinetic parameters as a function of initial solute concentration: New insight from adsorption of dye and heavy metals onto humic-like modified adsorbents. *Bull. Chem. React. Eng. Catal.* 16(4). 773-795. doi: 10.9767/bcrec.16.4.11816.773-795

[21] Yahya, M.D., Abubakar, H., Obayomi, K.S., Iyaka, Y.A., & Suleiman, B. 2020. Simultaneous and continuous biosorption of Cr and Cu (II) ions from industrial tannery effluent using almond shell in a fixed bed column. *Results Eng.* 6. 100113. doi: 10.1016/j.rineng.2020.10011

[22] Irawan, C., Dahlan, B., & Retno, N. 2021. The effect of adsorbent mass, contact time and adsorbent activation using hcl on the effectiveness of heavy metal (fe) reduction using fly ash as an adsorbent. *Jurnal Teknologi Terpadu*. 3(2). 89-96. doi: 10.32487/jtt.v3i2.89

[23] Haryanto, B., Sinaga, W.K., & Saragih, F.T. 2019. Study of interaction model on adsorption of heavy metal cadmium (Cd^{2+}) using black sand adsorbent. *Jurnal Teknik Kimia USU*. 8(2). 79-

84. doi: 10.32734/jtk.v8i2.2032
[24] Shi, Q., Terracciano, A., Zhao, Y., Wei, C., Christodoulatos, C., Meng, X. 2019. Evaluation of metal oxides and activated carbon for lead removal: kinetics, isotherms, column tests, and the role of co-existing ions. *Sci. Total Environ.* 648. 176–183. doi: 10.1016/j.scitotenv.2018.08.013
[25] Rahayu, I., Nazriati, Fajaroh, F. & Nur, A. 2019. Cadmium Ion Adsorption Using Bagasse-Based Silica Xerogel. *Journal Cis-Trans.* 3(1). 10-16. doi: 10.17977/um0260v3i12019p010